Journal of Nuclear Materials 376 (2008) 129–132

Contents lists available at ScienceDirect

Journal of Nuclear Materials

journal homepage: www.elsevier.com/locate/jnucmat

Preparation and characterisation of $Tl_2Pu(MoO_4)_3$ and $Tl_4Pu(MoO_4)_4$ in Tl–Pu–Mo–O system by X-ray and thermal methods

N.D. Dahale *, Meera Keskar, S.K. Sali, V. Venugopal

Fuel Chemistry Division, B.A.R.C. Trombay, Mumbai 400 085, India

ARTICLE INFO

Article history:
Received 1 January 2008
Accepted 31 January 2008

ABSTRACT

The quaternary Tl–Pu–Mo–O system was investigated for the first time and two new quaternary compounds $Tl_2Pu(MoO_4)_3$ and $Tl_4Pu(MoO_4)_4$ were synthesized by solid state reactions of Tl_2MoO_4 with $Pu(MoO_4)_2$ in 1:1 and 2:1 molar proportions at 773 K and 823 K, respectively. X-ray powder diffraction data of these compounds were indexed on orthorhombic system. Thermogravimetric (TG) curves of $Tl_2Pu(MoO_4)_3$ and $Tl_4Pu(MoO_4)_4$ were recorded in air and no significant weight changes were observed up to 973 K and 1033 K, respectively. Differential thermal analysis (DTA) curves of $Tl_2Pu(MoO_4)_3$ and $Tl_4Pu(MoO_4)_4$ showed endothermic peaks due to the melting of the compounds at 838 K and 1013 K, respectively. Non-isothermal kinetics of decomposition of $Tl_2Pu(MoO_4)_3$ and $Tl_4Pu(MoO_4)_4$ in air was studied using thermogravimetric technique. $Tl_2Pu(MoO_4)_3$ and $Tl_4Pu(MoO_4)_4$ when heated up to 1673 K decomposed to Tl_2O and MoO_3 in the gaseous form, giving solid PuO_2 as an end product. The reactions followed unimolecular nucleation and growth mechanism with activation energies of 106 kJ/mol and 157 kJ/mol, respectively.

1. Introduction

Rb, Cs and Mo are important fission products formed with large yield in a nuclear reactor during fission. Chemical interaction of these fission products among themselves as well as with nuclear fuel can lead to the formation of complex oxides, which may cause deformation and breaching of the fuel pins and also can change stoichiometry of the fuel oxide and thus affect the fuel behavior. Tabuteau et al. [1,2] and Katz et al. [3] studied alkali metal–plutonium–molybdenum–oxygen quaternary system by means of liquid–solid equilibrium diagrams and by X-ray diffraction, where compounds of the type $A_2Pu(MoO_4)_3$ and $A_4Pu(MoO_4)_4$, (A = Li, Na, K, Rb and Cs) were prepared and found to have scheelite and superscheelite structure, respectively. Tabuteau and Pages also studied $A_2^{I}MoO_4$–$A^{IV}(MoO_4)_2$ [A^{I} = K^+, Rb^+, Cs^+; A^{IV} = Np^{+4}, Pu^{+4}] and K_3MoO_4–Am_2^{III} $(MoO_4)_3$ system by micro thermal analysis and X-ray diffraction [4]. Huyghe reported the structural study of $K_2Th(MoO_4)_3$ and K_8Th $(MoO_4)_6$ and indexed them on monoclinic and triclinic systems, respectively [5,6]. Recently, we studied the crystal structure of $Na_2Th(MoO_4)_3$, $Na_2Pu(MoO_4)_3$, $Na_4Th(MoO_4)_4$, $Na_4Pu(MoO_4)_4$ [7] and $Na_2U(MoO_4)_3$, $Na_4U(MoO_4)_4$ [8] compounds by Rietveld profile method. It was established that $Na_2Th(MoO_4)_3$, $Na_2U(MoO_4)_3$ and $Na_2Pu(MoO_4)_3$ are isostructural having scheelite structure, whereas isostructural compounds $Na_4Th(MoO_4)_4$, $Na_4U(MoO_4)_4$ and $Na_4Pu(MoO_4)_4$ have superscheelite structure in tetragonal cell [7,8]. A study of pseudo-ternary phase diagram of Na_2O–UO_3–MoO_3 system was carried out by us and phase diagram was drawn using five quaternary compounds namely $Na_2UMo_2O_{10}$, $Na_2U_2Mo_2O_{13}$, $Na_2U_2Mo_3O_{16}$, $Na_2UMo_4O_{16}$ and $Na_2U_2Mo_4O_{19}$ [9].

As the ionic size of Tl^+(0.150 nm) is similar to that of Rb^+(0.152 nm), the compounds formed in these systems are expected to have similar properties [10]. Calorimetric and X-ray studies on $Tl_2(UO_2)_2(MoO_4)_3$ and $Tl_2Th(MoO_4)_3$ were carried out by us [11]. Even though much work has been carried out on Tl–Mo–O [12,13] and Pu–Mo–O systems [14], no work has been reported in quaternary thallium–plutonium–molybdenum–oxygen system. In Tl–Pu–Mo–O system, two novel compounds $Tl_2Pu(MoO_4)_3$ and $Tl_4Pu(MoO_4)_4$, were synthesised by solid state method and characterized by X-ray powder diffraction and thermal analysis techniques. The non-isothermal kinetic studies of decomposition of $Pu(MoO_4)_2$, $Tl_2Pu(MoO_4)_3$ and $Tl_4Pu(MoO_4)_4$ were also carried out using thermogravimetry.

2. Experimental

2.1. Preparation of $Tl_2Pu(MoO_4)_3$ and $Tl_4Pu(MoO_4)_4$

Tl_2MoO_4 and $Pu(MoO_4)_2$ were used as starting compounds for the synthesis of $Tl_2Pu(MoO_4)_3$ and $Tl_4Pu(MoO_4)_4$. Tl_2MoO_4 was prepared by heating a mixture of $Tl_2CO_{3(s)}$ and $MoO_{3(s)}$ in equimolar proportion in a platinum boat at 773 K for 20 h in air. $Pu(MoO_4)_2$ was prepared by heating a reaction mixture of PuO_2 and MoO_3 in 1:2 molar ratio in platinum boat in air initially at 773 K for 2 h

* Corresponding author. Fax: +91 22 25505151.
E-mail address: nddahale@barc.gov.in (N.D. Dahale).

0022-3115/$ - see front matter © 2008 Elsevier B.V. All rights reserved.
doi:10.1016/j.jnucmat.2008.01.028

and then at 1073 K for 15 h with intermittent grinding. The reaction is described by following equation:

$$PuO_2 + 2MoO_3 \xrightarrow{1073\ K} Pu(MoO_4)_2 \quad (1)$$

The formation of Tl_2MoO_4 and $Pu(MoO_4)_2$ were confirmed by comparing XRD data of the compounds with the data reported in literature [12,14].

$Tl_2Pu(MoO_4)_3$ and $Tl_4Pu(MoO_4)_4$ were prepared by reacting Tl_2MoO_4 and $Pu(MoO_4)_2$ in 1:1 and 2:1 molar proportion at 773 K and at 823 K, respectively. To get the homogeneous products, all the reaction mixtures were thoroughly mixed and ground in pestle and mortar before heating at desired temperature. The formation of these compounds is described by following equations:

$$Tl_2MoO_4 + Pu(MoO_4)_2 \xrightarrow{773\ K} Tl_2Pu(MoO_4)_3 \quad (2)$$

$$2Tl_2MoO_4 + Pu(MoO_4)_2 \xrightarrow{823\ K} Tl_4Pu(MoO_4)_4 \quad (3)$$

$Tl_2Pu(MoO_4)_3$ and $Tl_4Pu(MoO_4)_4$ were also synthesized by heating mixtures of Tl_2CO_3, PuO_2 and MoO_3 in stoichiometric ratios at 773 K and 823 K, respectively.

2.2. Instrumental analysis

The progress of the reactions and formation of $Tl_2Pu(MoO_4)_3$ and $Tl_4Pu(MoO_4)_4$ were monitored by recording XRD patterns on DIANO X-ray diffractometer using Cu Kα radiation (λ = 0.154178 nm). For the calculations of lattice parameters of the new product phases, XRD patterns of the compounds were recorded at the rate of 1/min.

Simultaneous Thermogravimetric (TG) and Differential Thermal Analysis (DTA) curves of $Pu(MoO_4)_2$, $Tl_2Pu(MoO_4)_3$ and $Tl_4Pu(MoO_4)_4$ were recorded on a Mettler Thermoanalyzer. The samples were heated in platinum cups in flowing stream of dry air. All the compounds were heated at the rate of 10 K/min up to 1673 K using sintered alumina as a reference material for DTA studies. To check the melting and solidification of $Pu(MoO_4)_2$, $Tl_2Pu(MoO_4)_3$ and $Tl_4Pu(MoO_4)_4$, compounds were heated up to 1223 K, 973 K and 1033 K, respectively and cooled to room temperature at the rate of 10 K/min. For each experiment, around 100 mg of sample was used.

Data for the radioactive samples of plutonium were recorded on DIANO X-ray diffractometer and Mettler Thermoanalyzer, both enclosed in glove boxes for handling radioactive materials.

3. Results and discussion

3.1. X-ray diffraction studies of $Tl_2Pu(MoO_4)_3$ and $Tl_4Pu(MoO_4)_4$

XRD data of $Pu(MoO_4)_2$ was indexed on orthorhombic system with lattice parameters a = 0.9422(5) nm, b = 1.0051(1) nm and c = 1.3986(2) nm which were in agreement with the reported data [14].

XRD data of $Tl_2Pu(MoO_4)_3$ and $Tl_4Pu(MoO_4)_4$ were indexed on the orthorhombic system and the cell parameters were refined by a least squares refinement method using a computer program [15]. XRD data of $Tl_2Pu(MoO_4)_3$ and $Tl_4Pu(MoO_4)_4$ were indexed on orthorhombic systems with lattice parameters a = 1.7737(10) nm, b = 1.2234(6) nm, c = 0.6644(2) nm and a = 1.1000(4) nm, b = 1.2076(5) nm, c = 0.9160(4) nm, respectively.

The refined cell parameters of $Pu(MoO_4)_2$, $Tl_2Pu(MoO_4)_3$ and $Tl_4Pu(MoO_4)_4$ are summarized in Table 1. The density of the compounds was determined by pycnometric method using toluene as a solvent. The measured and calculated densities are in good agreement and are included in Table 1, along with the number of molecules per unit cell.

The indexed XRD data of $Tl_2Pu(MoO_4)_3$ and $Tl_4Pu(MoO_4)_4$ are reported in Tables 2 and 3, respectively.

3.2. Thermal studies of $Pu(MoO_4)_2$, $Tl_2Pu(MoO_4)_3$ and $Tl_4Pu(MoO_4)_4$

Thermal behavior and non isothermal kinetics of $Pu(MoO_4)_2$, $Tl_2Pu(MoO_4)_3$ and $Tl_4Pu(MoO_4)_4$ were studied by TG/DTA curves.

TG curves of $Pu(MoO_4)_2$, $Tl_2Pu(MoO_4)_3$ and $Tl_4Pu(MoO_4)_4$ did not show significant weight losses up to 1223 K, 973 K and 1023 K, respectively. When heated up to 1673 K, thermograms of $Pu(MoO_4)_2$, $Tl_2Pu(MoO_4)_3$ and $Tl_4Pu(MoO_4)_4$ showed the decomposition from 1223 K, 973 K and 1033 K up to 1673 K and total observed weight losses were 46.72%, 75.34% and 82.50%, respectively. Final products in all the three decompositions were confirmed as PuO_2 by weight loss calculations and XRD. The observed weight losses were in good agreement with the theoretical weight losses for the formation of PuO_2 and are given in Table 4.

DTA curve of Plutonium molybdate $Pu(MoO_4)_2$ gave a sharp endothermic peak at 1223 K due to the melting of the compound. X-ray diffraction patterns of $Pu(MoO_4)_2$ before and after melting were identical. $Pu(MoO_4)_2$ when further heated up to 1473 K showed a weight loss of 46.7% forming PuO_2 as a end product and also confirmed by XRD.

Fig. 1 shows the DTA curve of $Tl_2Pu(MoO_4)_3$ obtained while heating up to 973 K, indicating a sharp endothermic peak at 838 K due to the melting of $Tl_2Pu(MoO_4)_3$. XRD pattern of the compound obtained before and after melting were identical. Melting of $Tl_2Pu(MoO_4)_3$ was confirmed by physical verification of the product. When $Tl_2Pu(MoO_4)_3$ was cooled at a controlled rate of 10 K/min, an exothermic DTA peak was observed at 733 K due to crystallization of the $Tl_2Pu(MoO_4)_3$.

To isolate the decomposition product, $Tl_2Pu(MoO_4)_3$ was heated outside in a furnace in air atmosphere at 973 K for 12 h, leading to the formation of a mixture of PuO_2, MoO_3 and $Tl_2Mo_2O_7$. The end product at 1673 K was identified as PuO_2. The decomposition sequence of $Tl_2Pu(MoO_4)_3$ is shown below

$$Tl_2Pu(MoO_4)_3 \xrightarrow{973\ K/air} Tl_2Mo_2O_7 + MoO_3 + PuO_2 \xrightarrow{1673\ K/air} Tl_2O\uparrow + 3MoO_3\uparrow + PuO_2 \quad (4)$$

DTA curve of $Tl_4Pu(MoO_4)_4$ gave a sharp endothermic peak at 1013 K due to the melting of $Tl_4Pu(MoO_4)_4$. The DTA curve obtained during the cooling showed an exothermic peak at 933 K due to the solidification of $Tl_4Pu(MoO_4)_4$. The difference between the melting and solidification temperatures in $Tl_2Pu(MoO_4)_3$ and $Tl_4Pu(MoO_4)_4$ may be due to the remaining of decomposition products in the melt or due to the super cooling of the liquid. Kinetically slow transitions results in super cooling or superheating during DTA runs. The lack of an internal equilibrium and unequal temperature distribution

Table 1
Crystal data of $Pu(MoO_4)_2$, $Tl_2Pu(MoO_4)_3$ and $Tl_4Pu(MoO_4)_4$

Compound	Crystal system	a (nm)	b (nm)	c (nm)	$\rho_{(cal.)}$ (g cm^{-3})	$\rho_{(obs.)}$ (g cm^{-3})	Z
$Pu(MoO_4)_2$	Orthorhombic	0.9422(5)	1.0051(1)	1.3986(2)	5.61	5.58	8
$Tl_2Pu(MoO_4)_3$	Orthorhombic	1.7737(10)	1.2234(6)	0.6644(2)	5.20	5.19	4
$Tl_4Pu(MoO_4)_4$	Orthorhombic	1.1000(4)	1.2076(5)	0.9160(4)	4.78	4.62	2

Table 2
XRD data of $Tl_2Pu(MoO_4)_3$ ($\lambda = 0.154178$ nm)

h	k	l	d_{obs} (nm)	d_{cal} (nm)	I/I_0
1	1	0	1.0051	1.0070	5
2	0	0	0.8875	0.8868	10
3	1	0	0.5334	0.5323	<5
2	2	0	0.5011	0.5035	<2
2	2	1	0.4026	0.4013	<5
0	1	2	0.3210	0.3206	10
1	1	2	0.3152	0.3155	100
5	1	1	0.3032	0.3032	15
6	0	0	0.2957	0.2956	15
3	4	0	0.2713	0.2716	5
7	0	1	0.2366	0.2367	5
3	3	2		0.2361	
2	1	3	0.2118	0.2116	10
0	6	1	0.1948	0.1949	<5
8	3	0		0.1948	
2	6	1	0.1903	0.1904	<5
0	4	3	0.1794	0.1794	<5
8	4	0		0.1795	
6	3	3	0.1626	0.1626	<5
4	7	0		0.1626	
2	2	4	0.1577	0.1577	10
2	6	3	0.1480	0.1480	<5
3	8	0		0.1479	

Table 3
XRD data of $Tl_4Pu(MoO_4)_4$ ($\lambda = 0.154178$ nm)

h	k	l	$d_{(obs)}$ (nm)	$d_{(cal)}$ (nm)	I/I_0
1	1	1	0.6102	0.60811	10
0	2	1	0.5035	0.5041	12
2	2	0	0.4083	0.4066	6
2	2	1	0.3715	0.3716	<5
1	2	2	0.3460	0.3463	16
3	1	1	0.3270	0.3276	100
0	0	3	0.3048	0.3053	25
2	0	3	0.2674	0.2669	<5
4	3	1	0.2200	0.2204	<5
2	2	3	0.2439	0.2442	11
1	5	1	0.2281	0.2285	20
0	5	3	0.1907	0.1894	38
3	2	4	0.1850	0.1849	13
2	6	1		0.1851	
0	0	5	0.1832	0.1832	10
5	3	3	0.1631	0.1632	6
4	6	1	0.1590	0.1599	<5
2	8	0	0.1456	0.1457	<5
0	6	5	0.1355	0.1355	40
6	6	0		0.1353	
8	1	3	0.1247	0.1247	<5

within the sample can also contribute to the phenomenon of differences in transition temperatures during heating and cooling, which was observed in $Na_2Pu(MoO_4)_3$, $Na_4Pu(MoO_4)_4$, $Na_2Th(MoO_4)_3$, $Na_4Th(MoO_4)_4$ [7], $Na_2U(MoO_4)_3$, $Na_4U(MoO_4)_4$ [8] and alkali metal uranyl molybdates [9].

XRD patterns obtained before and after cooling cycle of $Tl_4Pu(MoO_4)_4$ were different as $Tl_4Pu(MoO_4)_4$ starts decomposing after

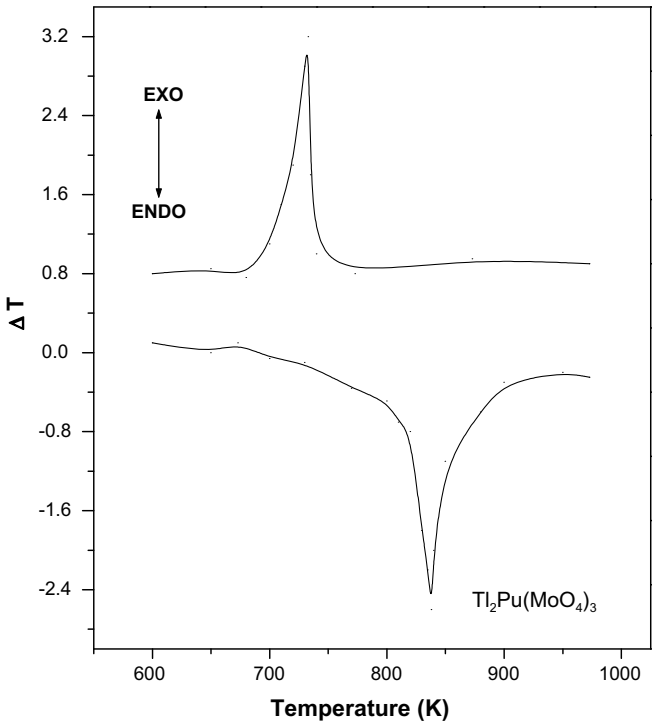

Fig. 1. DTA curves during heating and cooling cycle of $Tl_2Pu(MoO_4)_3$.

melting. $Tl_4Pu(MoO_4)_4$, when heated in the furnace at 1023 K for 12 h, disproportionate to a mixture of $Tl_2Mo_2O_7$ and PuO_2. As observed in $Tl_2Pu(MoO_4)_3$, heating of $Tl_4Pu(MoO_4)_4$ at 1673 K led to the formation of PuO_2 volatilizing Tl_2O and MoO_3, which was confirmed by weight loss calculations and XRD analysis of the end product. The decomposition sequence of $Tl_4Pu(MoO_4)_4$ is given below:

$$Tl_4Pu(MoO_4)_4 \xrightarrow{1033\ K/air} 2Tl_2Mo_2O_7 + PuO_2 \xrightarrow{1673\ K/air} 2Tl_2O\uparrow + 4MoO_3\uparrow + PuO_2 \quad (5)$$

3.3. Non-isothermal kinetics of $Pu(MoO_4)_2$, $Tl_2Pu(MoO_4)_3$ and $Tl_4Pu(MoO_4)_4$

Fig. 2 gives the plot of fraction reacted, α, against temperature for $Tl_2Pu(MoO_4)_3$ and $Tl_4Pu(MoO_4)_4$ along with MoO_3 and $Pu(MoO_4)_2$, where $\alpha = (W_t - W_o)/(W_\infty - W_o)$, W_t is the weight at temperature T, W_o is initial weight and W_∞ is the weight after completion of the reaction. These α vs. temperature plots display sigmoidal nature where initial rate of decomposition is very slow followed by gradually increasing decomposition rate up to a maximum and then slows down as the reaction approaches completion. The sigmoidal reaction kinetics is a characteristic of nucleation and growth mechanism. Fig. 2 also shows that the thermal stability of $Pu(MoO_4)_2$ is higher than those of $Tl_2Pu(MoO_4)_3$

Table 4
Thermal decomposition data of MoO_3, $Pu(MoO_4)_2$, $Tl_2Pu(MoO_4)_3$ and $Tl_4Pu(MoO_4)_4$ in air

Compound	Melting point (K)	Temperature range of decomposition (K)	End product	% Weight loss	
				Observed	Calculated
MoO_3	1068	1043–1550	–	100	100
$Pu(MoO_4)_2$	1223	1050–1500	PuO_2	46.72	50.70
$Tl_2Pu(MoO_4)_3$	838	1043–1553	PuO_2	75.34	75.95
$Tl_4Pu(MoO_4)_4$	1013	1033–1560	PuO_2	82.58	84.02

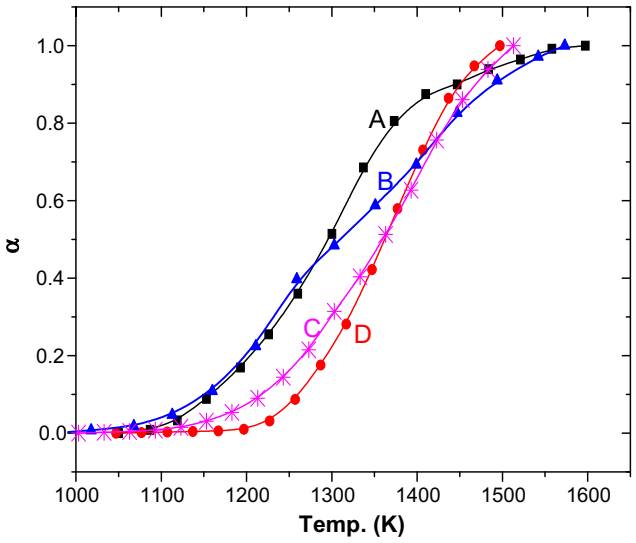

Fig. 2. α against temperature plot for (A) MoO_3, (B) $Tl_2Pu(MoO_4)_3$, (C) $Tl_4Pu(MoO_4)_4$ and (D) $Pu(MoO_4)_2$.

Table 5
Kinetic parameters for decomposition of MoO_3 and various plutonium molybdates

Reactant	Product	α range	Mechanism	Ea (kJ/mol)	Z $(s)^{-1}$
$Tl_2Pu(MoO_4)_3$	PuO_2	0.1–0.9	MAMP	106	1.5×10
$Tl_4Pu(MoO_4)_4$	PuO_2	0.1–0.9	MAMP	157	8.5×10^2
$Pu(MoO_4)_2$	PuO_2	0.1–0.9	MAMP	216	2.0×10^5
MoO_3	–	0.1–0.9	MAMP	136	2.9×10^2

MAMP: Nucleation and growth type, $g(\alpha) = -\ln(1-\alpha)$.

and $Tl_4Pu(MoO_4)_4$ and can also be seen from higher melting point of $Pu(MoO_4)_2$ as compared to thallium plutonium molybdates. When above compounds were heated in air, all these decomposed to give a solid product PuO_2. The kinetics of decomposition of a compound, where melting is followed by vaporization, has been reported in literature [16]. MoO_3 start volatilizing after melting at 1068 K. The volatilization of MoO_3 is at lower temperature than decomposition of $Tl_2Mo_2O_7$ forming Tl_2O and MoO_3 above 1100 K.

The procedure followed for obtaining kinetic parameters by non-isothermal method using thermogravimetric data has been reported earlier [16]. The kinetic data were calculated using computer program [17]. A typical computer output containing standard deviations for various mechanisms and activation energies for decomposition of $Tl_4Pu(MoO_4)_4$ to PuO_2 showed that lowest standard deviation occurred for nucleation and growth mechanism at an activation energy of 156 kJ/mol. Further iteration for smaller interval of activation energy was carried out which gave a value of 157 kJ/mol. Thus the decomposition of $Tl_4Pu(MoO_4)_4$ to PuO_2 is governed by unimolecular nucleation and growth (Mampel type) mechanism following the relation $g(\alpha) = -\ln(1-\alpha)$ [18]. Similarly decomposition of $Pu(MoO_4)_2$ and $Tl_2Pu(MoO_4)_3$ to PuO_2 followed unimolecular nucleation and growth mechanisms with an activation energy of 216 kJ/mol and 106 kJ/mol, respectively.

Table 5 gives kinetic parameters for decomposition of MoO_3 and various plutonium molybdates. It is observed that decomposition of all these compounds obeys first order kinetics indicating nucleation and growth as the rate-controlling step. Identical nature of α versus temperature plot of MoO_3 with those of $Tl_4Pu(MoO_4)_4$ and $Pu(MoO_4)_2$ indicates that the kinetics of decomposition of these compounds are controlled by MoO_3 volatilization.

4. Conclusion

In Tl–Pu–Mo–O system, two new quaternary compounds $Tl_2Pu(MoO_4)_3$ and $Tl_4Pu(MoO_4)_4$ were synthesised by solid state method and XRD data of the compounds were indexed on orthorhombic system. Ternary and quaternary compounds of thallium are not expected to form in nuclear reactor, but as Tl^+, K^+ and Rb^+ have close ionic radii, ternary or quaternary compounds in K–Pu–Mo–O and Rb–Pu–Mo–O system are expected to form similar compounds in nuclear reactor. $Tl_2Pu(MoO_4)_3$ and $Tl_4Pu(MoO_4)_4$ showed melting at 838 K and 1013 K, respectively followed by decomposition to PuO_2. The decomposition of these compounds showed unimolecular nucleation and growth mechanism with activation energies of 106 kJ/mol and 157 kJ/mol, respectively.

Acknowledgments

The authors are thankful to Dr.S. Kannan, Head, X-ray and Structural Studies Section for constant encouragement during this work and Dr. S. K. Aggarwal, Head, Fuel Chemistry Division for critical reading of the manuscript.

References

[1] A. Tabuteau, M. Pages, W. Freundlich, Mater. Res. Bull. 7 (1972) 691.
[2] A. Tabuteau, M. Pages, W. Freundlich, J. Inorg. Nucl. Chem. 42 (1980) 401.
[3] J.J. Katz, G.T. Seaborg, L.R. Morss (Eds.), The Chemistry of Actinide Elements, vol. I, Chapman and Hall, 1986, p. 720.
[4] A. Tabuteau, M. Pages, J. Solid State Chem. 26 (2) (1978) 153.
[5] M. Huyghe, M.R. Lee, Jaulmes, M. Quarton, Acta Crystallogr. C 49 (1993) 950.
[6] M. Huyghe, M.R. Lee, M. Quarton, F. Roben, Acta Crystallogr. C 47 (1991) 1797.
[7] N.D. Dahale, Meera Keskar, K.D. Singh Mudher, J. Alloy. Compd. 415 (2006) 244.
[8] N.D. Dahale, Meera Keskar, N.K. Kulkarni, K.D. Singh Mudher, J. Alloy. Compd. 440 (2007) 145.
[9] N.D. Dahale, Meera Keskar, R. Agarwal, K.D. Singh Mudher, J. Nucl. Mater. 362 (2007) 26.
[10] S. Dash, Z. Singh, N.D. Dahale, R. Prasad, V. Venugopal, J. Alloy. Compd. 302 (2000) 75.
[11] S. Dash, Z. Singh, N.D. Dahale, R. Prasad, V. Venugopal, J. Alloy. Compd. 347 (2002) 301.
[12] M. Touboul, P. Toledano, C. Idoura, E.M.M. Bolze, J. Solid State Chem. 61 (1986) 354.
[13] M. Touboul, C. Idoura, P. Toledano, Acta Crystallogr. C 40 (1984) 1652.
[14] R. Roof, Los Alamos National laboratory Report (LAUR) 11619 3 (1991) 1027.
[15] V.K. Wadhavan, LATPAR, A Least Squares Program, Neutron Physics Division, Bhabha Atomic Research Centre, Mumbai, India.
[16] K. Krishnan, G.A. Rama Rao, K.D. Singh Mudher, V. Venugopal, J. Nucl. Mater. 230 (1996) 61.
[17] P.V. Ravindran, Thermochim. Acta. 39 (1980) 135.
[18] S.K. Mukerjee, J.V. Dehadraya, V.N. Vaidya, D.D. Sood, J. Nucl. Mater. 172 (1990) 37.